crystals

MDPI

Communication

A Simple Dip-Coating Method of SnO_2-NiO Composite Thin Film on a Ceramic Tube Substrate for Methanol Sensing

Tianyu Liu [1], Longxiao Xu [1], Xiangyue Wang [2], Qiuyang Li [3], Qiang Cui [3], Hui Suo [1,*] and Chun Zhao [1,*]

1 State Key Laboratory of Integrated Optoelectronics, College of Electronic Science and Engineering, Jilin University, Changchun 130118, China; liuty17@mails.jlu.edu.cn (T.L.); xulx18@mails.jlu.edu.cn (L.X.)
2 College of Chemistry, Jilin University, Changchun 130118, China; xiangyue18@mails.jlu.edu.cn
3 College of Electronic Science and Engineering, Jilin University, Changchun 130118, China; liqy@mails.jlu.edu.cn (Q.L.); cuiqiang@mails.jlu.edu.cn (Q.C.)
* Correspondence: suohui@jlu.edu.cn (H.S.); zchun@jlu.edu.cn (C.Z.)

Received: 2 November 2019; Accepted: 25 November 2019; Published: 26 November 2019

Abstract: In this work, SnO_2-NiO composite thin film was successfully grown on a ceramic tube substrate directly by a simple dip-coating method combined with annealing. Characterization analysis demonstrates that uniform SnO_2 film consists of a great number of nanospheres and NiO grows on SnO_2 as an agglomerated block. In comparison to the pure SnO_2 sample, the SnO_2-NiO composite thin films gas sensor exhibits superior methanol sensing properties at 225 °C. The gas response to 10 ppm methanol reached 15.12 and the response and recovery times were 8 s and 7 s, respectively. The excellent selectivity and recovery rate are explained by the unique properties of the NiO semiconductor and the higher sensor response is attributed to the pivotal heterojunction effect.

Keywords: SnO_2-NiO composite; gas sensor; methanol; dip-coating; heterojunction

1. Introduction

SnO_2 is a typical wide band-gap (Eg = 3.6 eV) n-type semiconductor and has been widely used in the gas sensor field owing to the advantage of its low cost, stable electrical properties, excellent physical and chemical stability and unique optical performance [1–3]. However, pure SnO_2 gas sensors have several limitations such as poor selectivity [4], slow recovery [5] and high working temperature [6]. To date, many researchers have taken measures to improve its gas sensing performance, such as doping various elements and compositing several sensing materials [7,8]. In addition, an effective strategy which has been effectively demonstrated to control the carrier concentration and enhance the response is to construct heterojunctions among different semiconductor oxides [9,10]. Additionally, NiO is a typical p-type semiconductor with a 3.5 eV band gap and has been widely considered as an excellent additive to improve response/recovery speeds and stability [11]. Therefore, the combination of nickel oxide and tin dioxide materials has been investigated in several reports [12,13]. However, coating ceramic tubes with the powders is a necessary step in the fabrication of gas sensors, which leads to poor repeatability because the thickness cannot be controlled. Therefore, a direct growth process on ceramic tubes could solve this problem perfectly.

Methanol is one of the toxic gases among volatile organic compounds, and has been widely used in the production of formaldehyde, colorings and antifreeze [14]. Furthermore, it can be processed into fuel cells in automobiles as a clean form of energy [15]. However, small amounts of methanol may cause blindness and fatal diseases [16]. Therefore, a methanol gas sensor with low detection

limit, high response and fast response and recovery rate is essential in daily life. At present, numerous research workers are contributing to research on methanol sensing. G. Korotcenkov et al. fabricated Au-modified SnO_2 films through a successive ionic layer deposition method, which exhibits a high response to 50 ppm methanol [17]. A CdS-doped tin oxide thick film made up by Lallan et al. [18] employing a screen-printing technology has a 70 response and 100 s recover time to 5000 ppm methanol. Song et al. [19] reported a hierarchical tin oxide nanoflower structure by hydrothermal synthesis and showed a high response (58) as well as low operating temperature (200 °C) to 100 ppm methanol. Although they have achieved a high response to methanol associated with a fast response rate and low working temperature, their detection limit is more than 50 ppm, which motivates us to prepare a new gas sensor with an outstanding sensing performance combined with a low detection limit.

Herein, we prepared a complete SnO_2-NiO composite thin film on a gas sensing ceramic tube directly through a dip-coating method, which avoided the cumbersome coating process and brought a repeatable growth technic. A comparative methanol response examination between SnO_2 and SnO_2-NiO composite is subsequently performed. The results of gas sensing measurements show that SnO_2-NiO composite thin film (SnO_2–NiO TF) possesses a prominent enhancement in selectivity, recovery rate (7 s) and gas response (15.12). Compared with previous work on methanol sensors, the SnO_2-NiO composite thin film gas sensor exhibited a lower detection limit combined with high response, fast response (18 s) and recovery rate and excellent selectivity. The improvement mechanism regarding the decoration of NiO is also discussed.

2. Materials and Methods

All chemicals (analytical grade reagents) were obtained from Beijing Chemical Works (Beijing, China) without further purification. The preparation process of SnO_2-NiO TF on the ceramic substrate was as follows: Firstly, in order to obtain $Sn(OH)_4$ sol, 130 uL of citric acid (0.1 M) was added to a 100 mL solution of $SnCl_4$ (0.13 M) and 0.1 M ammonia solution was added dropwise to raise the solution pH to 2. The resulting product was centrifuged, and the precipitate was added into 50 mL deionized water. The ammonia solution was added drop by drop to the mixed solution under magnetic stirring at 50 °C until the pH value was adjusted to 9. Secondly, the preparation of $Ni(OH)_2$ sol: 3.7326 g $Ni(CH3COO)_2{\cdot}4H_2O$ and 5 g PEG6000 was dissolved in 100 mL ethanol and the mixed solution was stirred continuously for 1 hour at 60 °C. Then, 10 mL of 25% ammonia was added dropwise and the resulting product was stirred at 70 °C for 1 day. Thirdly, ceramic tube substrates were dipped into the $Sn(OH)_4$ sol for approximately 60 s and then, they were removed at a rate of 50 um/s. To avoid cracks in the $Sn(OH)_4$ coating, the specimen was first dried at ambient temperature for 60 minutes and heated at 100 °C in a muffle furnace for about 60 minutes. The dip-coating process was repeated 3 times and the specimen was maintained at 500 °C for 2 hours to obtain tin dioxide thin film. After that, the dip-coating process and parameters of NiO were the same as those of SnO_2.

The crystal structure information of the SnO_2-NiO TF on a ceramic substrate were characterized through X-ray diffraction (XRD, Rigaku D/Max 2550, Rigaku, Ltd, Tokyo, Japan) with a Cu Kα radiation line of 0.1506 nm at 40 kV, 200 mA. The Field Emission Electron Microscopy (FESEM, JEOL JSM-7500 F, JEOL, Ltd, Tokyo, Japan) was used to determine the microstructure and morphology of the specimen. In addition, the bonding state of SnO_2 and NiO was observed by means of the Transmission Electron Microscope (TEM, JEOL JEM-3010, JEOL, Ltd, Tokyo, Japan). In this paper, the Pt wires on as-prepared ceramic tubes and heating wires were welded to the bases and aged at 200 °C for 2 days to form gas sensor devices (Figure 1a). Besides, the static working system was used to measure the response of the gas sensor and is shown in Figure 1b. In detail, the device was placed in a 2.5 L as-prepared air chamber, and the resistance data was transferred to a Fluke 8846A digital multimeter connected to the computer. Furthermore, the heating wire inside the ceramic tube was used in conjunction with GPD3303S and the target gas was injected into the air chamber through a syringe. During the measurement, the Fluke 8846 Arecorded one resistor per second and displayed the data on the computer for real-time monitoring. The gas response was defined as S = Ra/Rg, in which Ra was the electrical resistance in

the air chamber and Rg was that in the target gas environment. The response and recovery time were defined as the time taken to reach 90% of the final stable resistance change value.

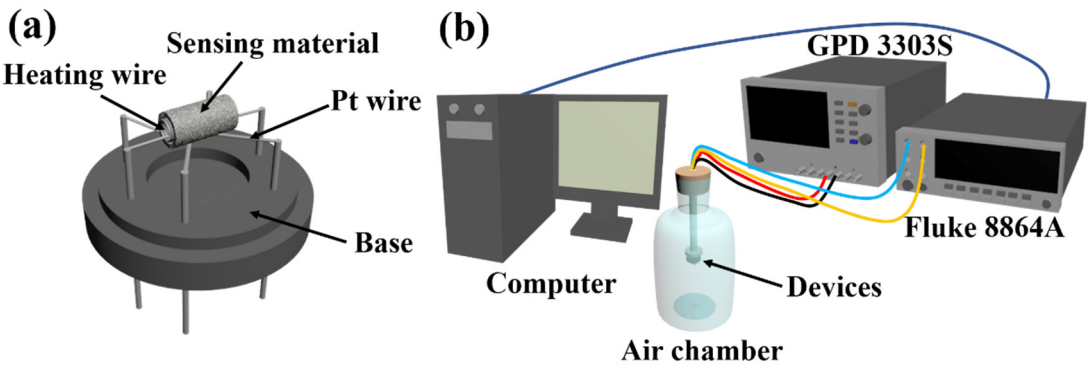

Figure 1. Schematic drawing of (**a**) as-prepared sensor device (**b**) measuring system of gas sensors.

3. Results and Discussion

The crystallographic information of SnO_2-NiO TF on a ceramic tube substrate and pure ceramic substrate has been obtained out by X-ray diffraction analysis. The results are presented in Figure 2. Obviously, all the diffraction peaks of the ceramic substrate can be easily associated to the standard peak values of Al_2O_3 (JCPDS No.10-173) and SiO_2 (JCPDS No.1-438), which indicates that these two oxides are the main component of the substrate. Furthermore, the diffraction peaks appearing at 26.86° and 34.08° can be indexed to SnO_2 (JCPDS No.2-1337), which confirms that SnO_2 has successfully grown on the ceramic tube substrate. However, the peaks of NiO do not appear in the sample, which is probably due to the low NiO concentration on the surface. For the purpose of confirming the crystal structure of NiO in the sample, as a comparison, pure NiO powder was obtained by heating the $Ni(OH)_2$ sol-gel to a temperature of 500 °C, and X-ray diffraction analysis was carried out. The diffraction peaks of this material are in good agreement with NiO (JCPDS No.4-835) and the diffraction peak at 43.27° is also the observed in the diffraction pattern of Al_2O_3, which is another reason for that NiO is not detected.

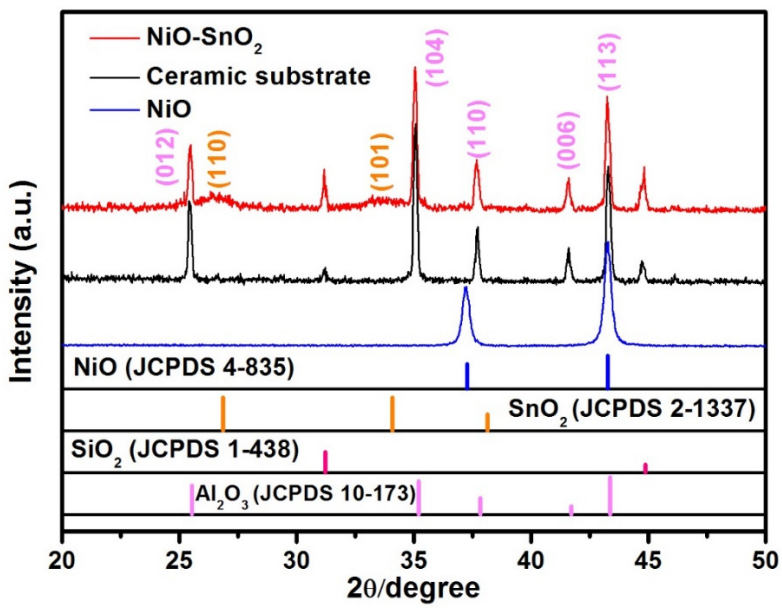

Figure 2. XRD pattern of the as-prepared SnO_2-NiO thin film (TF), ceramic substrate and NiO powders.

The morphology and structure of pure SnO_2 and SnO_2-NiO TF on the ceramic tube substrate are shown in Figure 3. Compared with the surface of the pure ceramic tube in Figure 3a, a smooth film structure has appeared on the surface in Figure 3b. Combined with the result of XRD, the thin film consisted of SnO_2, and the further details could be seen in Figure 3c, in which tiny SnO_2 nanoparticles were found to be tightly stacked together. This aggregation mode may prevent the internal tin dioxide from contacting methanol and only conduct charge transfer, which is not conducive to increasing the sensitivity. The image in Figure 3d indicated that the thickness of SnO_2 is about 301.5 nm. Moreover, we could see that NiO grows on SnO_2 as an agglomerated block in Figure 3e. The high-magnification picture (Figure 3f) indicates the contact gap of NiO nanoparticles is larger than that of SnO_2, which can provide a more reactive site to methanol. The low magnification of SnO_2-NiO TF on the ceramic tube observed in Figure 3g exhibits a smooth and uniform surface of SnO_2-NiO TF. In order to obtain the particle morphology of tin oxide and nickel oxide, the sample is characterized by using TEM and Figure 3h reveals that the particle diameter of SnO_2 and NiO is about 8–9 nm. Further details of the lattice structure can be observed in Figure 3i through the high-resolution TEM image (HRTEM). A lattice spacing of 0.331 nm and 0.264 nm matches the SnO_2 planes of (110) and (101), respectively [20,21], and the lattice spacing of 0.240 nm is the same as the NiO plane of (111) [22].

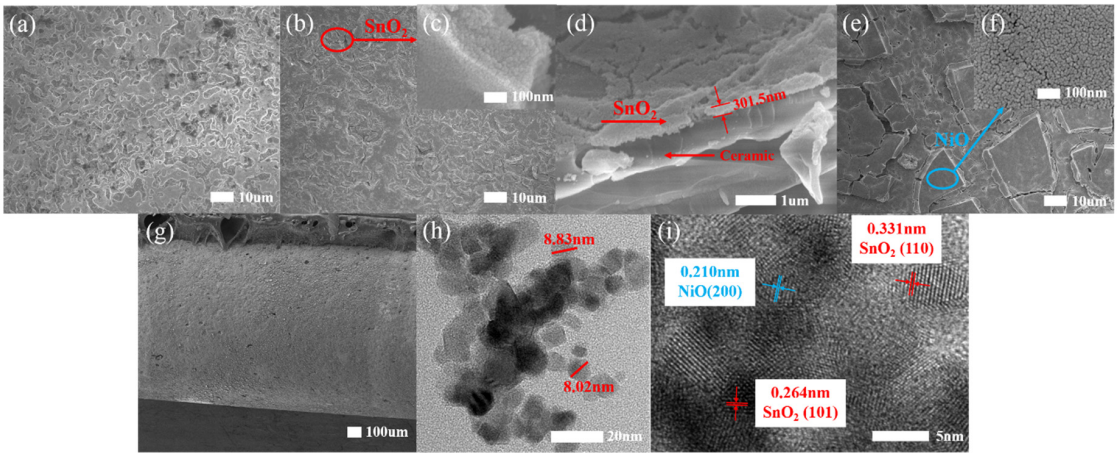

Figure 3. FESEM images of (**a**) the ceramic substrate (**b**–**d**) pure SnO_2 on the ceramic substrate and (**e**–**g**) SnO_2-NiO TF on the ceramic substrate; TEM images of (**h**,**i**) the SnO_2-NiO composite.

The gas sensors performance under different operation temperatures was also tested. Figure 4a displays the gas response of pure SnO_2 and SnO_2-NiO TF sensors in 10 ppm methanol at varying operating temperatures from 100 to 375 °C. The two response curves in this chart reveal that the maximum response of SnO_2 and SnO_2-NiO TF is observed under the optimal operating temperature of 225 °C, with the response values being 4.5 and 15.12, respectively. The two curves also show that the decoration of NiO evidently improves the response to methanol. The selectivity of sensors to 10 ppm of various gases was also investigated. Figure 4b indicates that the pure SnO_2 sensor has similar responses to most of the test gases. On the other hand, compared with other gases, the SnO_2-NiO TF gas sensor reveals an outstanding response to methanol, which indicates that SnO_2-NiO TF has a unique selectivity to methanol and the decoration of NiO must play a vital role in this process. Figure 4c shows the sensor response to 10 ppm methanol at 225 °C with seven reversible cycles. This chart demonstrates both sensors exhibit an outstanding repeatability. Figure 4d indicates that the response time of both sensors to 10 ppm methanol are 18 s and the recovery times of pure SnO_2 and SnO_2-NiO TF sensors are 7 s and 15 s, respectively. The improvement of the recovery time may be attributed to the heterojunction formed between NiO and SnO_2. The dynamic response curves of both gas sensors exposed to methanol gas in the concentration range from 0.1 to 100 ppm at 205 °C is shown in Figure 4e. According to the curve, the response increases rapidly and with good linearity to methanol in the range of 1–100 ppm. The minimum concentration that the sensors are capable of

detecting is around 1 ppm. Figure 4f also indicates the responses of pure and SnO_2-NiO TF sensors to a wide range of 1–1000 ppm vs. a narrow range of 1–100 ppm of methanol. Above 100 ppm, the response of the sensors increases more slowly, which reveals a saturated trend to methanol. The superb linear relationship under 100 ppm indicates that this sensor is better at detecting low concentrations of methanol. Besides, the long-term stability in Figure 4g indicated an excellent performance of both sensors. In order to offer a contrast with other published results, a comparison of methanol gas-sensing characteristics using other compounds in previous reports is listed in Table 1. Evidently, the SnO_2/NiO thin film in this work exhibits a remarkable response to 10 ppm methanol, combined with a lower operating temperature and faster recovery time than the others.

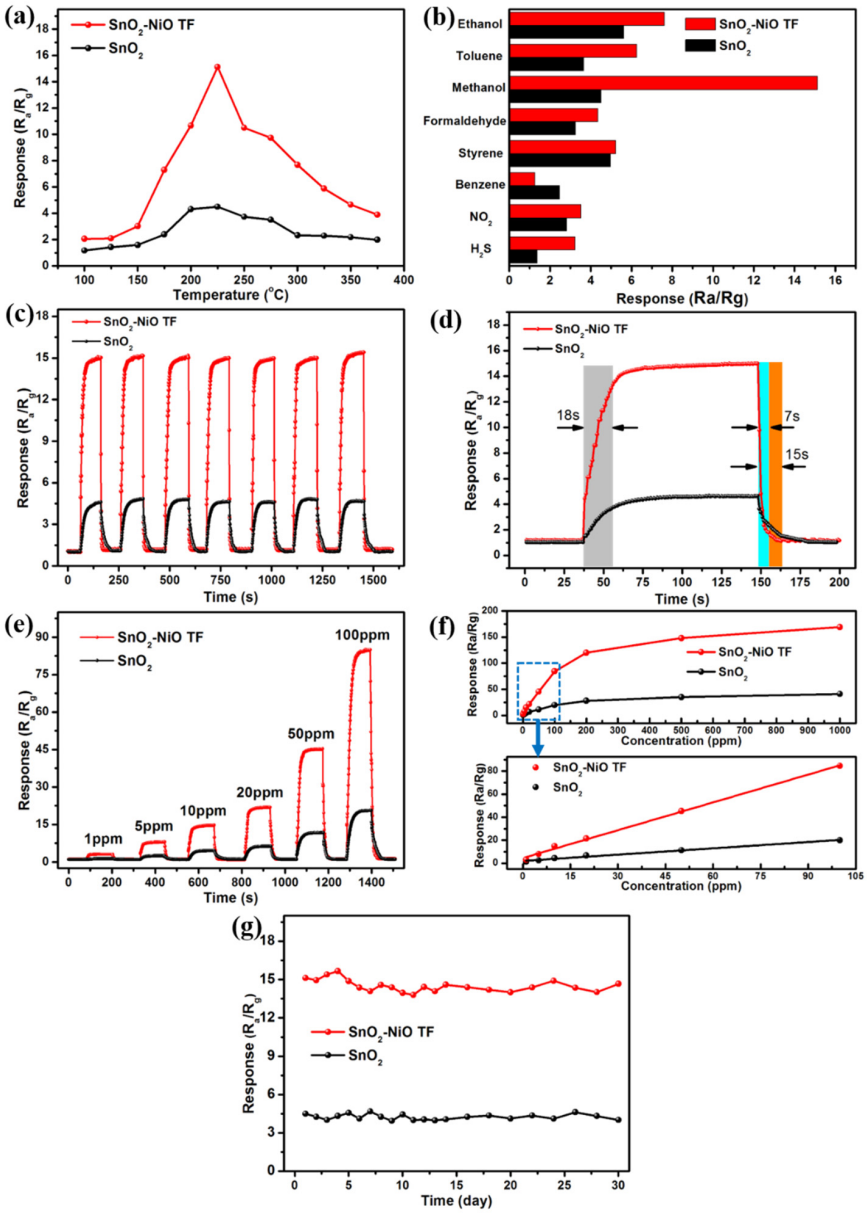

Figure 4. (**a**) Responses of pure and SnO_2-NiO TF sensors at various working temperatures to 10 ppm methanol, (**b**) selectivity to 10 ppm various gases, (**c**) seven reversible cycles to 10 ppm methanol at 225 °C, (**d**) dynamic response and recover property to 10 ppm methanol, (**e**) the dynamic response change toward 1–100 ppm methanol, (**f**) the response of sensors to 1–1000 ppm methanol and fitting line of the response in range of 1–100 ppm methanol, (**g**) long-term stability of sensors to 10 ppm methanol.

Table 1. Comparison of methanol gas-sensing characteristics using other compounds in previous reports.

Sensing Material	Concentration (ppm)	Temperature (°C)	Response	Response/Recovery Time	Reference
Au decorated ZnO	10	300	2.7	~20 s/~15 s	[23]
ZnO-SnO_2 nanostructure microspheres	10	300	~2	~18 s/~35 s	[24]
SnO_2-ZnO composites nanofibers	10	350	8.5	20 s/40 s	[25]
α-Fe_2O_3 hollow spheres	10	280	25.1	8 s/9 s	[26]
SnO_2/ZnO nanofibers	10	350	~8.9	~12 s/~31 s	[27]
GaN nanostructures	10	350	~1.3	~15 s/~30 s	[28]
CuO nanoparticles	10	220	5.9	13 s/13 s	[29]
Zn doping SnO_2 nanorods clusters	10	270	11.5	~10 s/~10 s	[30]
three-dimensionally $LaFeO_3$	10	190	~2	~12 s/~15 s	[31]
honeycomb-like SnO_2	10	320	~4	~20 s/~20 s	[32]
SnO_2/NiO thin film	10	225	15.12	18 s/7 s	This work

Similarly to other semiconductors, the gas-sensing mechanism of the SnO_2-NiO composite thin film to methanol shown in Figure 5a relies on the adsorption and desorption of oxygen, which leads to a change in the resistance [33–35]. Furthermore, the good selectivity and fast recovery rate are attributed to the unique properties of p-type semiconductors such as NiO [36]. Specifically, the methanol decomposition temperature on the surface of the NiO material is 240 °C [37], which is slightly higher than our operating temperature, while leading to the accumulation of methanol and good selectivity. The improvement of gas sensitivity achieved by SnO_2-NiO TF to methanol is probably attributed to a heterojunction effect and is exhibited in Figure 5b. In detail, the p–n heterojunction is formed between NiO and SnO_2. In general, the Fermi energy of SnO_2 is different from that of NiO, which leads to a temporary relative movement of charge carriers at the interface of both semiconductors until a new balance is achieved. During this process, the space charge layer is generated and the phenomenon of energy band bending in the depletion layer increases the barrier height and exhibits a higher resistance. When exposed to methanol, the adsorbed oxygen will remove electrons from methanol molecules rapidly and previous electrons will be absorbed back into SnO_2 and NiO, which results in an increase of the area of electric transport channels. As a result, the resistance of the SnO_2-NiO TF gas sensor in methanol decreased and the gas response increased. Furthermore, a great number of cracks on the surface of nickel oxide also provide more reaction sites for methanol.

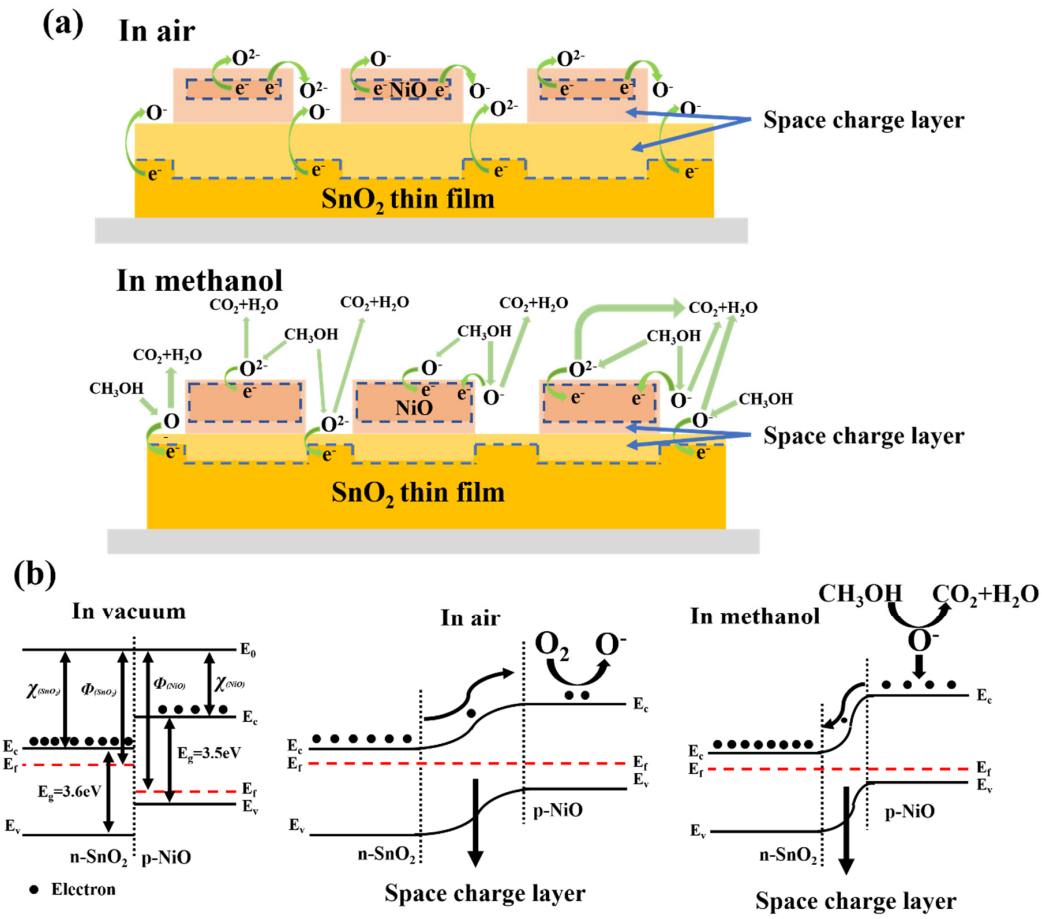

Figure 5. (**a**) The changes of the space charge layer of SnO_2-NiO TF when exposed to air and methanol. (**b**) The energy band diagram of contact between NiO and SnO_2 in air and methanol.

4. Conclusions

In summary, a highly sensitive gas sensor is realized by decorating an agglomerated block of NiO on an SnO_2 thin film, which delivers outstanding performances for the detection of methanol. Herein, XRD, SEM and TEM patterns indicated that NiO nanoparticles have been successfully attached onto the SnO_2 films. As for the gas-sensitive performance to methanol, the SnO_2 gas sensor exhibits a better selectivity, recovery time and gas response than pure SnO_2. The sensing improvement realized by the NiO composite, in addition to special properties of the NiO semiconductor, can be attributed to the heterojunction effect between NiO and SnO_2, resulting in an increase of the gas response.

Author Contributions: Conceptualization, T.L. and X.W.; methodology, L.X.; investigation, Q.L. and Q.C.; writing—original draft preparation, T.L.; writing—review and editing, T.L.; providing the gas sensing mechanism, H.S. and C.Z.

Funding: This work is financially supported by National Natural Science Foundation of China (Grant NOs. 61474056 and 51672103).

Conflicts of Interest: The authors declare no conflict of interest.

References

1. Choi, K.-I.; Hübner, M.; Haensch, A.; Kim, H.-J.; Weimar, U.; Barsan, N.; Jong, H.-L. Ambivalent effect of Ni loading on gas sensing performance in SnO_2 based gas sensor. *Sens. Actuators B Chem.* **2013**, *183*, 401–410. [CrossRef]
2. Ge, Q.; Ma, S.Y.; Xu, Y.B.; Xu, X.L.; Chen, H.; Qiang, Z.; Yang, H.M.; Ma, L.; Zeng, Z. Preparation, characterization and gas sensing properties of Pr-doped ZnO/SnO_2 nanoflowers. *Mater. Lett.* **2017**, *191*, 5–9. [CrossRef]
3. Rongjun, Z.; Xu, Z.; Sijia, P.; Ping, H.; Tong, Z.; Zidong, W.; Xinxin, X.; Yue, Y.; Yude, W. Shaddock peels as bio-templates synthesis of Cd-doped SnO_2 nanofibers: A high performance formaldehyde sensing material. *J. Alloy. Compd.* **2020**, *813*, 152170.
4. Park, K.-R.; Cho, H.-B.; Lee, J.; Song, Y.; Kim, W.-B.; Choa, Y.-H. Design of highly porous SnO_2-CuO nanotubes for enhancing H_2S gas sensor performance. *Sens. Actuators B Chem.* **2020**, *302*, 127179. [CrossRef]
5. Yinglin, W.; Chang, L.; Lian, W.; Jie, L.; Bo, Z.; Yuan, G.; Peng, S.; Yanfeng, S.; Tong, Z.; Geyu, L. Horseshoe-shaped SnO_2 with annulus-like mesoporous for ethanol gas sensing application. *Sens. Actuators B Chem.* **2017**, *240*, 1321–1329.
6. Van Hieu, N.; Kim, H.-R.; Ju, B.-K.; Lee, J.-H. Enhanced performance of SnO_2 nanowires ethanol sensor by functionalizing with La_2O_3. *Sens. Actuators B Chem.* **2008**, *133*, 228–234. [CrossRef]
7. Kang, W.; Tianyu, Z.; Gang, L.; Qinqin, Y.; Chunhong, L.; Qilong, W.; Deliang, C. Room temperature CO sensor fabricated from Pt-loaded SnO_2 porous nanosolid. *Sens. Actuators B Chem.* **2013**, *184*, 33–39. [CrossRef]
8. Miao, Y.-E.; He, S.; Zhong, Y.; Yang, Z.; Tjiu, W.W.; Liu, T. A novel hydrogen peroxide sensor based on Ag/SnO_2 composite nanotubes by electrospinning. *Electrochim. Acta* **2013**, *99*, 117–123. [CrossRef]
9. Shouli, B.; Ke, T.; Hang, F.; Yongjun, F.; Ruixian, L.; Dianqing, L.; Aifan, C.; Chung, C.L. Novel α-Fe_2O_3/$BiVO_4$ heterojunctions for enhancing NO_2 sensing properties. *Sens. Actuators B Chem.* **2018**, *268*, 136–143.
10. Shi, S.; Zhang, F.; Lin, H.; Wang, Q.; Shi, E.; Qu, F. Enhanced triethylamine-sensing properties of P-N heterojunction Co_3O_4/In_2O_3 hollow microtubes derived from metal–organic frameworks. *Sens. Actuators B Chem.* **2018**, *262*, 739–749. [CrossRef]
11. Xiaoguang, S.; Guodong, Z.; Guosheng, W.; Yanbai, S.; Dan, M.; Yajing, Z.; Fanli, M. Assembly of 3D flower-like NiO hierarchical architectures by 2D nanosheets: Synthesis and their sensing properties to formaldehyde. *RSC Adv.* **2017**, *7*, 3540–3549.
12. Jahromi, H.S.; Behzad, M. Construction of 0, 1, 2 and 3 dimensional SnO_2 nanostructures decorated by NiO nanopetals: Structures, growth and gas-sensing properties. *Mater. Chem. Phys.* **2018**, *207*, 489–498. [CrossRef]
13. Zhang, L.; He, J.; Jiao, W. Synthesis and gas sensing performance of NiO decorated SnO_2 vertical-standing nanotubes composite thin films. *Sens. Actuators B Chem.* **2019**, *281*, 326–334. [CrossRef]
14. Kun, L.; Yinzhen, W.; Mingpeng, C.; Qian, R.; Zhongqi, Z.; Qingju, L.; Jin, Z. High Methanol Gas-Sensing Performance of Sm_2O_3/ZnO/$SmFeO_3$ Microspheres Synthesized Via a Hydrothermal Method. *Nanoscale Res. Lett.* **2019**, *14*, 57.
15. Qing, L.; Tanyuan, W.; Dana, H.; Hanguang, Z.; Ping, X.; Jiantao, H.; Jaephil, C.; Gang, W. High-Performance Direct Methanol Fuel Cells with Precious-Metal-Free Cathode. *Adv. Sci.* **2016**, *3*, 1600140.
16. Mengting, Z.; Yuxin, Y.; Chang, L.; Peiyi, H.; Song, H.; Liancheng, Z.; Xianshun, Z. A colorimetric and fluorometric dual-modal sensor for methanol based on a functionalized pentacenequinone derivative. *Chem. Commun.* **2018**, *54*, 8339–8342.
17. Korotcenkov, G.; Brinzari, V.; Gulina, L.B.; Cho, B.K. The influence of gold nanoparticles on the conductivity response of SnO_2-based thin film gas sensors. *Appl. Surf. Sci.* **2015**, *353*, 793–803. [CrossRef]
18. Yadava, L.; Verma, R.; Dwivedi, R. Sensing properties of CdS-doped tin oxide thick film gas sensor. *Sens. Actuators B Chem.* **2010**, *144*, 37–42. [CrossRef]
19. Liming, S.; Anatolii, L.; Denys, B.; Haibo, L.; Junkai, Z.; Ming, F.; Liying, L.; Duo, C.; Klyui, N.I. Facile Synthesis of Hierarchical Tin Oxide Nanoflowers with Ultra-High Methanol Gas Sensing at Low Working Temperature. *Nanoscale Res. Lett.* **2019**, *14*, 84.
20. Li, Z.; Yi, J. Enhanced ethanol sensing of Ni-doped SnO_2 hollow spheres synthesized by a one-pot hydrothermal method. *Sens. Actuators B Chem.* **2017**, *243*, 96–103. [CrossRef]

21. Kim, J.; Mirzaei, H.A.; Kim, H.W.; Kim, S.S. Variation of shell thickness in ZnO-SnO_2 core-shell nanowires for optimizing sensing behaviors to CO, C_6H_6, and C_7H_8 gases. *Sens. Actuators B Chem.* **2020**, *302*, 127150. [CrossRef]
22. Sikai, Z.; Yanbai, S.; Pengfei, Z.; Jin, Z.; Wei, Z.; Xiangxiang, C.; Dezhou, W.; Ping, F.; Yansong, S. Highly selective NO_2 sensor based on p-type nanocrystalline NiO thin films prepared by sol–gel dip coating. *Ceram. Int.* **2018**, *44*, 753–759.
23. Xianghong, L.; Jun, Z.; Liwei, W.; Taili, Y.; Xianzhi, G.; Shihua, W.; Shurong, W. 3D hierarchically porous ZnO structures and their functionalization by Aunanoparticles for gas sensors. *J. Mater. Chem.* **2011**, *21*, 349–356.
24. Li, C.C.; Yin, X.M.; Li, Q.H.; Wang, T.H. Enhanced gas sensing properties of ZnO/SnO_2 hierarchical architectures by glucose-induced attachment. *CrystEngComm* **2011**, *13*, 1557–1563. [CrossRef]
25. Tang, W.; Wang, J.; Yao, P.; Li, X. Hollow hierarchical SnO_2-ZnO composite nanofibers with heterostructure based on electrospinning method for detecting methanol. *Sens. Actuators B Chem.* **2014**, *192*, 543–549. [CrossRef]
26. Yang, H.M.; Ma, S.Y.; Yang, G.J.; Jin, W.X.; Wang, T.T.; Jiang, X.H.; Li, W.Q. High sensitive and low concentration detection of methanol by a gas sensor based on one-step synthesis α-Fe_2O_3 hollow spheres. *Mater. Lett.* **2016**, *169*, 73–76. [CrossRef]
27. Tang, W. Sensing mechanism of SnO_2/ZnO nanofibers for CH_3OH sensors: Heterojunction effects. *J. Phys. D Appl. Phys.* **2017**, *50*, 475105. [CrossRef]
28. Ji, H.-F.; Liu, W.-K.; Li, S.; Li, Y.; Shi, Z.-F.; Tian, T.Y.; Li, X.-J. High-performance methanol sensor based on GaN nanostructures grown on silicon nanoporous pillar array. *Sens. Actuators B Chem.* **2017**, *250*, 518–524. [CrossRef]
29. Fang, W.; Hairong, L.; Zhaoxin, Y.; Yongzhe, S.; Fangzhi, C.; Heng, D.; Longzhen, X.; Haiyan, L. A highly sensitive gas sensor based on CuO nanoparticles synthetized via a sol–gel method. *RSC Adv.* **2016**, *6*, 79343–79349.
30. Ding, X.; Zeng, D.; Xie, C. Controlled growth of SnO2 nanorods clusters via Zn doping and its influence on gas-sensing properties. *Sens. Actuators B Chem.* **2010**, *149*, 336–344. [CrossRef]
31. Qin, J.; Cui, Z.; Yang, X.; Zhu, S.; Li, Z.; Liang, Y. Synthesis of three-dimensionally ordered macroporous $LaFeO_3$ with enhanced methanol gas sensing properties. *Sens. Actuators B Chem.* **2015**, *209*, 706–713. [CrossRef]
32. Wang, L.L.; Li, Z.J.; Luo, L.; Zhao, C.Z.; Kang, L.P.; Liu, D.W. Methanol sensing properties of honeycomb-like SnO_2 grown on silicon nanoporous pillar array. *J. Alloy. Compds.* **2016**, *682*, 170–175. [CrossRef]
33. Cai, Z.-X.; Li, H.-Y.; Ding, J.-C.; Guo, X. Hierarchical flowerlike WO_3 nanostructures assembled by porous nanoflakes for enhanced NO gas sensing. *Sens. Actuators B Chem.* **2017**, *246*, 225–234. [CrossRef]
34. Chen, H.; Wang, Q.; Kou, C.; Sui, Y.; Zeng, Y.; Du, F. One-pot synthesis and improved sensing properties of hierarchical flowerlike SnO_2 assembled from sheet and ultra-thin rod subunits. *Sens. Actuators B Chem.* **2014**, *194*, 447–453. [CrossRef]
35. Li, L.; Yu, Z.; Guoguang, W.; Shouchun, L.; Lianyuan, W.; Yu, H.; Xiaoxue, J.; Aiguo, W. High toluene sensing properties of NiO-SnO_2 composite nanofiber sensors operating at 330 °C. *Sens. Actuators B Chem.* **2011**, *160*, 448–454. [CrossRef]
36. Geng, X.; Lahem, D.; Zhang, C.; Li, C.-J.; Olivier, M.-G.; Debliquy, M. Visible light enhanced black NiO sensors for ppb-level NO_2 detection at room temperature. *Ceram. Int.* **2019**, *45*, 4253–4261. [CrossRef]
37. Badlani, M.; Wachs, I.E. Methanol: A "Smart" Chemical Probe Molecule. *Catal. Lett.* **2001**, *75*, 137. [CrossRef]